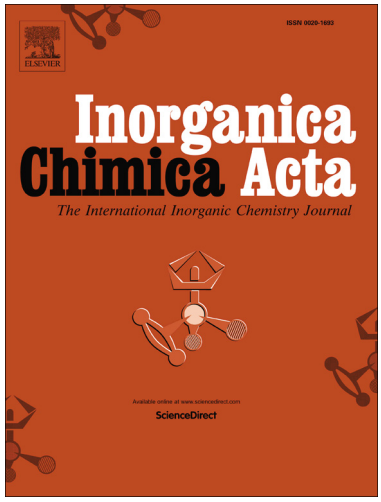

Research paper

Synthesis, characterization, anticancer and antibacterial evaluation of Schiff base ligands derived from hydrazone and their transition metal complexes

Roghayeh Fekri, Mehdi Salehi, Asadollah Asadi, Maciej Kubicki

PII: S0020-1693(18)30782-5
DOI: https://doi.org/10.1016/j.ica.2018.09.022
Reference: ICA 18480

To appear in: *Inorganica Chimica Acta*

Received Date: 19 May 2018
Revised Date: 16 August 2018
Accepted Date: 8 September 2018

Please cite this article as: R. Fekri, M. Salehi, A. Asadi, M. Kubicki, Synthesis, characterization, anticancer and antibacterial evaluation of Schiff base ligands derived from hydrazone and their transition metal complexes, *Inorganica Chimica Acta* (2018), doi: https://doi.org/10.1016/j.ica.2018.09.022

Synthesis, characterization, anticancer and antibacterial evaluation of Schiff base ligands derived from hydrazone and their transition metal complexes

Roghayeh Fekri[a], Mehdi Salehi[a,*], Asadollah Asadi[b], Maciej Kubicki[c]

[a] *Department of Chemistry, College of Science, Semnan University, Semnan, Iran*

[b]*Department of Biology, Faculty of Science, University of Mohaghegh Ardabili, Ardabil, Iran*

[c]*Faculty of Chemistry, Adam Mickiewicz University, Umultowska 89b, 61-614 Poznan, Poland*

Correspondence:Email: msalehi@semnan.ac.ir

Abstract

Copper(II), Nickel(II) and Cobalt(III) complexes with Schiff base ligands derived from hydrazone, (**HL^1** = (E)-N'-(pyridin-2-ylmethylene)benzohydrazide, **H_2L^2** = (E)-2-(2-hydroxybenzylidene)hydrazine-1-carboxamide and **HL^3** = (E)-2-(pyridin-2-ylmethylene)hydrazine-1-carboxamide, were synthesized and spectroscopically characterized by FT-IR, ^{1}H NMR, UV-Vis spectroscopy, X-ray crystallography and cyclic voltammetry. The synthesized compounds have been screened for their antibacterial activities against the bacterial species E. coli, K. pneumonia (Gram-negative) and S. aureus, B. subtilis (Gram-positive) by minimum inhibitory concentration (MIC) and minimum bactericidal concentration (MBC) methods. In vitro anticancer studies of the ligands and coordination compounds (**1-3**) using MTT assay was also done. Results show that the complexes (**1-3**) have higher antibacterial and anticancer activities than the respective free ligands.

Keywords: Hydrazone, Spectral properties, Crystal Structure, Antibacterial study, Anticancer activity.

1. Introduction

Schiff base complexes have continued to play the role of one of the most important stereochemical models in transition metal coordination chemistry due to their structural versatility associated with various applications [1-4]. In analytical chemistry, hydrazones are prepared by the reaction of aldehydes with hydrazines. They can act as multidentate ligands with transition metals and show many applications [5]. Hydrazone compounds bearing ONO and NNO donor atoms have been introduced to coordination chemistry [6-7]. Hydrazones have physiological and biological activities such as anticancer [8], antibacterial [9], antioxidant [10], antifungal [11], anti-tubercular [12] and anti-inflammatory [13]. There has

been considerable interest in copper, cobalt and nickel Schiff base complexes derived from hydrazones [14-19]. Base on today studies, the design and synthesis of new metal-based cancer chemotherapeutic agents, is in the most important part of the research area in inorganic medicinal chemistry. Several recent articles have summarized the anticancer activity of metal complexes derived from hydrazones such as cobalt, nickel and copper complexes. Moreover, a series of hydrazone derivatives were synthesized and screened for antibacterial activity against Gram-positive and Gram-negative bacteria [20-25, 27]. In this paper, metal chelates of Schiff base derived from hydrazones have been prepared (Scheme 1). Schiff base ligands were synthesized and identified as described before [26-28]. Single crystal X-ray crystallography studies confirm that the Schiff bases act as tridentate ligands. The free ligands and their complexes (**1-3**) are screened for their antibacterial activities against Gram-positive and Gram-negative bacteria. Further, the cytotoxic effect of the compounds examined on AGS and SW742 cancer cell lines. The purpose of this study is to compare the biological activities of the synthesized compounds (**1-3**) and their respective ligands.

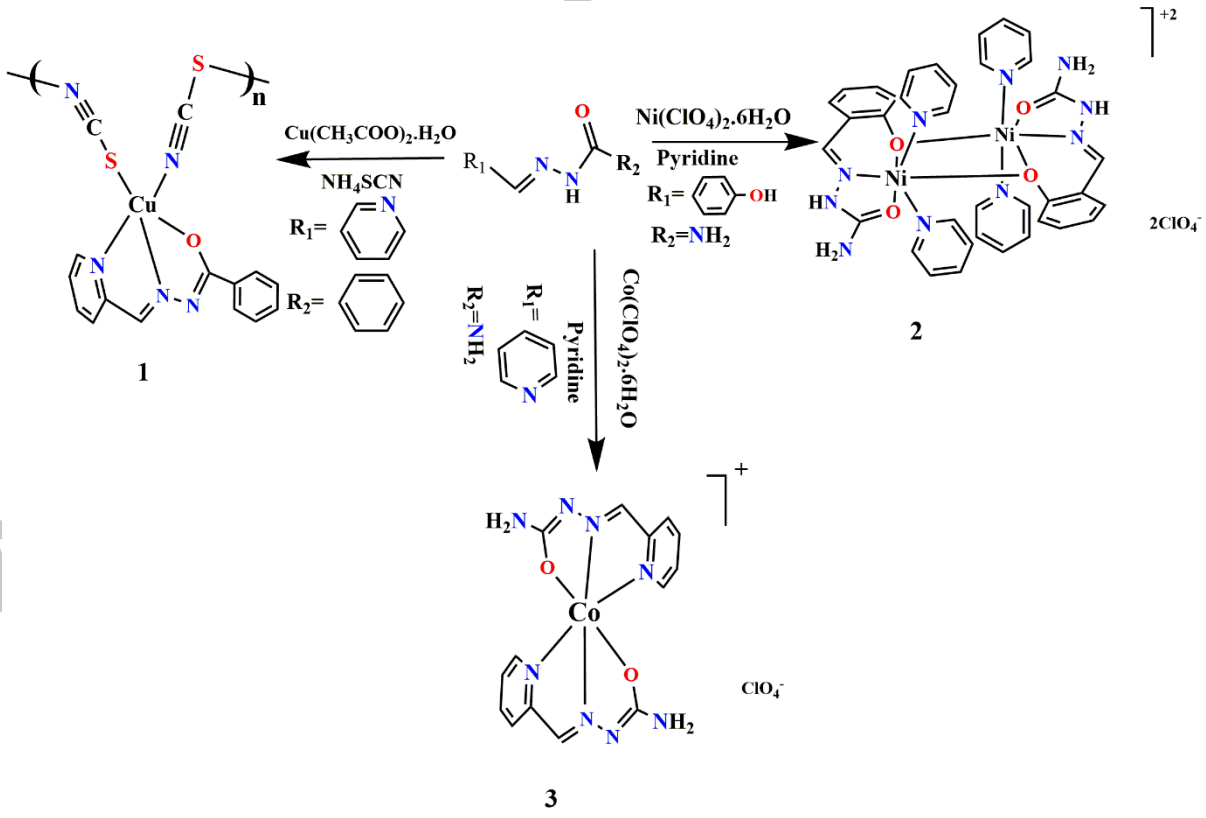

Scheme 1. Schematic depiction of complexes (**1-3**).

2. Experimental

2.1 Materials and instrumentation

All solvents and chemicals were purchased from commercial sources and used without purification. FT-IR spectra (KBR disks) were recorded on a Bruker spectrophotometer. Shimadzu UV-1650PC spectrophotometer was used to record the electronic spectra of compounds. ^{1}HNMR measurements were carried out on BRUKER AVANCE DR X400 (400 MHz) spectrometer at room temperature. Cyclic voltammetric measurements have been performed on metrohm 757 VA computerace. RPMI 1640 and fetal bovine serum (FBS) were obtained from Gibco. Phosphate-buffered saline (PBS)**,** dimethylsulfoxide (DMSO), dimethylformamide (DMF) and other chemicals were purchased from Sigma-Aldrich.

2.2 Synthesis of HL^1

A mixture of an ethanolic solution of benzohydrazide (10 mmol) and pyridinecarbaldehyde (10 mmol) was refluxed for 3 h. Then, the yellow precipitate was filtered and washed with cold ethanol [26]. Yield: 85%. M. P. = 183 ºC. FT-IR: ν_{max} cm^{-1} (KBr): 1621 (C=O), 1603 (C=N). UV-Vis: λ_{max} (nm) (ε, M^{-1} cm^{-1}) (Methanol): 282 (3980), 328 (3040).

2.3 Synthesis of H_2L^2

An ethanol solution of hydrazinecarboxamide (10 mmol) was added to an ethanol solution of salicylaldehyde (10 mmol) and the mixture was refluxed for 4h. The resulting light yellow precipitate was filtered off and washed with cooled ethanol [27]. Yield: 75%. M. P. = 161 ºC. FT-IR: ν_{max} cm^{-1} (KBr): 1681 (C=O), 1612 (C=N). UV-Vis: λ_{max} (nm) (ε, M^{-1} cm^{-1}) (Methanol): 303 (4410), 329 (5480).

2.4 Synthesis of HL^3

The synthesis of **HL^3** was performed using the same procedure for **H_2L^2** with pyridinecarbaldehyde instead of salicylaldehyde. The white precipitate of the ligand was obtained [28]. Yield: 70%. M. P. = 172 ºC. FT-IR: ν_{max} cm^{-1} (KBr) 1689 (C=O), 1667 (C=N). UV-Vis: λ_{max} (nm) (ε, M^{-1} cm^{-1}) (Methanol): 287 (3680), 307 (3850).

2.5 Synthesis of complexes (1-3)

2.5.1 Synthesis of $[Cu^{II}(L^1)(SCN)_2]_n$ (1)

The (E)-N'-(pyridin-2-ylmethylene)benzohydrazide ligand, **HL^1**, (0.5 mmol) was dissolved in methanol (10 ml) and after adding of $Cu(CH_3COO)_2.H_2O$ (0.5 mmol) and NH_4SCN (1 mmol), the resulting solution was refluxed for 4 h. After 4 days, crystals of the complex were

appeared, filtered off, washed with methanol and air dried. Yield: 54%. FT-IR: ν_{max} cm^{-1} (KBr) 1591 (C=N). UV-Vis: λ_{max} (nm) (ε, M^{-1} cm^{-1}) (Methanol): 353 (4300).

2.5.2 Synthesis of $[Ni^{II}_2(L^2)_2(Py)_4].2ClO_4$ (2)

$Ni(ClO_4)_2.6H_2O$ (0.5 mmol) in 10 ml of methanol was added to a stirred solution of (E)-2-(2-hydroxybenzylidene)hydrazine-1-carboxamide, $\mathbf{H_2L^2}$, (0.5 mmol) in 10 ml of methanol. Then, to this solution pyridine (1 ml) was added and the mixture was refluxed for 3h. The crystals were obtained after 5 days. Yield: 64%. FT-IR: ν_{max} cm^{-1} (KBr) 1596 (C=N). UV-Vis: λ_{max} (nm) (ε, M^{-1} cm^{-1}) (Methanol): 373 (1920). ^{1}H-NMR (DMSO-d^6, 400 MHz): 7.56, 7.76 (s, 2H, CH=N), 7.90-8.37 (s, 4H, H_2N), 6.55-7.42 (m, 31H, ArH).

2.5.3 Synthesis of $[Co^{III}(L^3)_2].ClO_4$ (3)

To a stirring solution of $Co(ClO_4)_2.6H_2O$ (0.5 mmol) in methanol (20 ml) an equimolar amount of (E)-2-(pyridin-2-ylmethylene)hydrazine-1-carboxamide, $\mathbf{HL^3}$, was added. To this solution pyridine (1 ml) was added and the air was bubbled through the reaction and refluxed for 4 h. The crystals of **3** suitable for X-ray crystallography were obtained after 3 days. Yield: 68%. FT-IR: ν_{max} cm^{-1} (KBr): 1603 (C=N). UV-Vis: λ_{max} (nm) (ε, M^{-1} cm^{-1}) (Methanol): 314 (3660). ^{1}H-NMR (DMSO-d^6, 400 MHz): 7.91, 7.92 (s, 2H, CH=N), 8.01-9.92 (s, 4H, H_2N), 6.77-11.38 (m, 8H, ArH).

2.6 X-ray crystallography

Diffraction data were collected by the ω-scan technique at 130(1) K (**1**, **3**) on Rigaku SuperNova four-circle diffractometer with Atlas CCD detector and mirror-monochromated CuK_α radiation (λ=1.54178 Å) and at 100(1) K (**2**), on Rigaku Xcalibur four-circle diffractometers with Eos CCD detector and graphite-monochromated MoK_α radiation (λ=0.71069 Å). The data were corrected for Lorentzian and polarization as well as for absorption effects [29]. Precise unit-cell parameters were determined by a least-squares fit of 4026 (**1**), 4770 (**2**), and 4689 (**3**) reflections of the highest intensity, chosen from the whole experiment. The structures were solved with SHELXT-2013 and refined with the full-matrix least-squares procedure on F^2 by SHELXL-2013 [30]. All non-hydrogen atoms were refined anisotropically, hydrogen atoms were placed in idealized positions and refined as 'riding model' with isotropic displacement parameters set at 1.2 times U_{eq} of appropriate carrier atoms. Table 1 lists the relevant experimental data and refinement details.

Crystallographic data for the structural analysis has been deposited with the Cambridge Crystallographic Data Centre, Nos. CCDC-1811093 (**1**), CCDC-1811094 (**2**), and CCDC-1811095 (**3**). Copies of this information may be obtained free of charge from: The Director, CCDC, 12 Union Road, Cambridge, CB2 1EZ, UK. Fax: +44(1223)336-033, E-mail: deposit@ccdc.cam.ac.uk, or www.ccdc.cam.ac.uk.

"TABLE 1"

2.7 Cyclic voltammetry

Cyclic voltammetric measurements were performed using a three-electrode system (Ag/AgCl as reference electrode, glassy carbon as working electrode, platinum wire as an auxiliary electrode) under a nitrogen atmosphere at 25 °C and using tetrabutylammonium hexafluorophosphate as supporting electrolyte (complex concentrations of about 1×10^{-3} M in DMF solution).

2.8 In vitro antibacterial efficiency

The Schiff base ligands and compounds (**1-3**) were tested against four different bacteria species: Escherichia coli (PTCC-1270), Klebsiella pneumonia (PTCC-1053) as Gram-Negative bacteria and Staphylococcus aureus (PTCC-1112) and Bacillus subtilis (PTCC-1254) as Gram-Positive bacteria. The antibacterial activities of (**1-3**) were compared with their respective ligands. The minimal inhibitory concentration (MIC) and the minimum bactericidal concentration (MBC) data of the synthesized compounds were given in Table 4. The Broth macro-dilution method was used to measure the MIC by a LB broth. The contents in the tubes were mixed thoroughly and incubated overnight at 37°C. The MIC is the lowest concentration of compound that produces inhibition of bacterial growth and MBC is the lowest concentration of antibiotic required to kill a particular bacterium. It determined from broth dilution minimum inhibitory concentration (MIC) tests by sub culturing to Mueller-Hinton agar plates and incubated at 37 °C for overnight [31-33]-. Kanamycin and Co-trimoxazole were of standard antibacterial agents included in the test [34-35].

2.9 In vitro anticancer activity

Anticancer effect of compounds were assayed by MTT assay against human gastric cancer (AGS) and human colon cancer (SW742) cell lines. The cytotoxicity of compounds (**1-3**) was compared with the ligands. The assay is based on the reduction of soluble yellow tetrazolium

salt to insoluble purple formazan crystals in the presence of enzyme in the mitochondria of the live cells. For this assay, cells were seeded into a 96 well plates at a density of 1×10^5 cells per ml in 0.2 mL of culture medium (RPMI 1640 with 10% fetal bovine serum (FBS)), then incubated at 37 °C. After 24h the culture medium was replaced by RPMI 1640 medium with different concentrations of the **HL^1, H_2L^2, HL^3**, **1**, **2**, and **3** (0.125, 0.25, 0.5, 1 and 2 mg/ml) and incubated at 37 °C for 24 h. Percentage cell viability was determined by MTT assay [36-39].

3. Result and Discussion

3.1 Synthesis and characterization

Three new complexes (**1-3**) of copper, nickel and cobalt have been synthesized. All the synthesized compounds were characterized on the basis of spectral data and X-ray crystallography data suggest that the **1**, **2** and **3** complexes are polymer-coordinated, binuclear and mononuclear Schiff base complexes, respectively.

3.2 IR spectra

Some important infrared absorption frequencies of the ligands and complexes (**1-3**) are presented here. All the free Schiff base ligands show characteristic azomethine at 1603 cm^{-1} for **HL^1**, 1612 cm^{-1} for **H_2L^2** and 1667 cm^{-1} for **HL^3**. The former shifts towards the lower frequency in the spectra of complexes at 1591, 1596 and 1603 cm^{-1} for **1**, **2** and **3**, respectively, are due to involvement of the N atom of the -C=N- group in coordination. Strong band at 2002 cm^{-1} is due to the SCN group for **1**. The appearance of some new bands in the FT-IR spectra of (**1-3**) in the regions 606-641 and 621-751 cm^{-1} are probably due to M-N and M-O bands, respectively.

3.3 Electronic spectra

The electronic absorption spectra of methanolic solution (1×10^{-4} M) of ligands and complexes (**1-3**) were recorded at 200-800 nm wavelength range and at 298 K. The bands at 228, 227 and 254 nm are attributable to intraligand $\pi\rightarrow\pi^*$ transitions of the benzene ring in **HL^1**, **H_2L^2** and **HL^3**, respectively. **HL^1**, **H_2L^2** and **HL^3** ligands show intensity bands at 282, 303 and 287 nm, respectively, which are assigned as $\pi\rightarrow\pi^*$ transition of the C=N and these bands in the electronic spectra of (**1-3**), are shifted as a result of coordination and appeared at 353 nm for **1**, 373 nm for **2** and 314 nm for **3**. Also, the electronic spectrum of ligands

exhibited bands at 328, 329 and 307 nm which assigned to $n \rightarrow \pi^*$ for **HL**^{1}, **H$_2$L**^{2} and **HL**^{3}, respectively and these bands disappeared upon chelation. For the all the synthesized compounds (**1-3**), d-d transitions probably appeared in the area under the charge transfer.

3.4 X-Ray studies

The polymeric structure (**1**) and structure of complexes (**2-3**) are shown in Figs. (1-6). The polymeric structure (**1**) is a second polymorphic form of this compound; the first one was published recently [40]. The first one was published recently. Both forms are $P2_1$ monoclinic, and the monomer look quite similarly in both cases (Fig. 1a), but the conformation of polymeric chain is different [40]. In published structure the subsequent monomers are almost perpendicular while in (**1**) they are parallel (Fig. 1b). This difference is a consequence of different construction of the polymer: in XIQLIT consecutive monomers are related by 2_1 screw axis, which in (**1**) – by unit-cell translation along x. Cu cation is 5-coordinated in square-pyramid environment (Table 2, Fig. 2). N1A, N8A, O10A and N1B atoms are approximately coplanar (max deviation 0.046(10Å), S1B(-1+x,y,z) is 2.8278(11)Å above this plane and Cu1 is slightly, by 0.1476(10) Å, displaced towards S atom. The ligand molecule is almost planar, Table 2 lists the dihedral angles between the approximately planar fragments. In the crystal structure, the neighbouring polymeric chains are connected – besides van der Waals interactions - only by weak C-H···S hydrogen bond contacts (H···S distance 2.87Å). In **2** a dication $Ni_2L_2(Py)_4$ (bridged by the oxygen atoms of ligand molecule, Fig. 3) is C_i-symmetrical, occupying the special position on the inversion center in the space group $I2/a$. The Ni atoms are six-coordinated in quite regular octahedral fashion. In the crystal structure the perchlorate anions neutralize the cation charge and take part in the hydrogen bond system, which involves also NH groups and C_2-symmetrical water molecule (Table 3 lists the details of hydrogen bonds). It can be noted, that the second hydrogen atom from NH_2 group, not involved in intermolecular N-H···O hydrogen bond system, strengthens the supramolecular architecture by taking part in relatively short and directional intermolecular N-H···π hydrogen bond (Fig. 4, Table 3). Complex (**3**) contains monocation CoL_2 and perchlorate counterion. Co ion is six-coordinated, again in octahedral geometry (Fig. 5, Table 2). The N-H···N and N-H···O hydrogen bonds connect molecules into infinite chains connected by centrosymmetric dimers created by $R^2_2(8)$ and $R^4_4(12)$ hydrogen-bond motifs (Fig. 6, Table 3).

"Fig. 1"

"Fig. 2"

"Fig. 3"

"Fig. 4"

"Fig. 5"

"Fig. 6"

"TABLE 2"

"TABLE 3"

3.5 Electrochemical studies

Cyclic voltammetry analysis of complexes was recorded in DMF solution. As shown in Fig. 7 (a), tow redox peaks emerge at -0.65V attributed to the cathodic and at 0.36 V attributed to the anodic peak, corresponding to the transfer of $Cu^{(II)}/Cu^{(I)}$ and $Cu^{(I)}/Cu^{(II)}$ states for (**1**), respectively. Fig. 7 (b) describes the cyclic voltammetric behavior of complex (**2**). The cyclic voltammogram of this complex presented reduction peaks in the potential of -0.77 and -0.65 V that are assigned to $Ni^{(II)}/Ni^{(I)}$ and there is not any clear oxidative peak for (**2**). Also the voltammetric response in Fig. 7 (c), for complex (**3**), is attributed to redox process include a cathodic peak at -0.45V and an anodic peak at 0.40 V, corresponding to the transfer of $Co^{(III)}/Co^{(II)}$ and $Co^{(II)}/Co^{(III)}$.

"Fig. 7"

3.6 ^{1}H NMR

Further evidence for the presence of coordinated Schiff base ligands in the new complexes is provided by the ^{1}H NMR spectra of the complexes. In complexes (**2**) and (**3**) the signals due to the azomethine proton (CH=N) appeared as a singlet at 7.56 and 7.76 ppm and 7.91, 7.92 ppm, respectively. Signals appeared in the 6.55-7.42 ppm region for (**2**) and 6.77-11.38 ppm for (**3**) has been assigned to the phenyl ring and pyridine protons. Also in the complexes (**2**) and (**3**) NH_2 protons appeared between 7.90-8.37 ppm and 8.01-9.92 ppm, respectively.

3.7 Antibacterial activity

The synthesized ligands and synthesized compounds (**1-3**) were tested for in vitro antimicrobial activity. They are tested against the bacteria; Escherichia coli, Klebsiella pneumonia, (Gram-Negative bacteria) and Staphylococcus aureus, Bacillus subtilis, (Gram-Positive bacteria). The minimum inhibitory concentration (MIC) and the minimum bactericidal concentration (MBC) values of the compounds against bacteria are summarized in Table 4. A comparative study of MIC and MBC values of ligands and compounds (**1-3**) indicate that the synthesized compounds (**1-3**) exhibit higher antimicrobial activity than the respective free ligands against Gram-Positive bacteria [41]. Increased activity of compounds can be illustrated on the basis of the Tweedy's chelation theory [42]. The reduction in polarity increases the lipophilic character of the chelates. This may cause the formation of hydrogen bonded interaction through the coordinated anions and azomethine group with the active centers. These properties may be used in metal transport across the bacterial membranes or to attach to the bacterial cells at a specific site from which it can interfere their growth. Thus, based on obtained results, the antimicrobial activity of the compounds (**1-3**) shows greater activity compared to their respective ligands [43].

"TABLE 4"

3.8 Cytotoxicity assay

In vitro anticancer activities of the synthesized Schiff base ligands and compounds (**1-3**) were tested by MTT assay against AGS and SW742 cell lines. The AGS and SW742 cells were incubated in the presence of increasing concentrations of the synthesized compounds. The results of these experiments were shown in Figs. 8 and 9. The absorbance was measured at 570 nm and the cell viability (%) was calculated according to the following equation:

$$\text{Cell viability (\%)} = \frac{OD_{570(sample)}}{OD_{570(control)}} \times 100$$

Where $OD_{570(sample)}$ and $OD_{570(control)}$ represent the absorbance values of the cells treated and control cells, respectively. From the results, it can be seen that all the synthesized compounds (**1-3**) have higher activities than the respective free ligands due to the presence of metal moieties and chelation in the compounds [44-45]. Figs. 8 and 9 show relationship between AGS and SW741 cells viability (%) and the reciprocal concentration of ligands and their metal compounds. Based on the results, upon increasing the concentration of test compounds, all the compounds have a good increase in cytotoxic potencies. The activity of the synthesized compounds (**1-3**) and their respective ligands show that all compounds (**1-3**) have better activity than respective ligands against AGS and SW174 cancer cell lines. The increase in

biological activities of the metal chelates such as anticancer and antibacterial may be due to the effect of the metal ion on the normal cell process. A possible mode of toxicity increase may be considered in the light of Tweedy, s chelation theory [46]. Chelation considerably reduces the polarity of the metal ion because of partial sharing of its positive charge with the donor group and possible π-electron delocalization within the whole chelate ring system that is formed during coordination. Such chelation could enhance the lipophilic character of the central metal atom and hence increase the hydrophobic character and liposolubility of the complex favoring its permeation through the lipid layers of the cell membrane.

"Fig. 8"

"Fig. 9"

3.9 Conclusion

Three novel complexes of copper, nickel and cobalt obtained by hydrazone Schiff base ligands. Ligands and their metal compounds have been characterized with FT-IR, ^{1}HNMR and UV-Vis spectroscopy. Electrochemical studies of the compounds (**1-3**) indicate that metal compounds show redox behavior. Single crystal X-Ray analysis reveals that the compounds **1**, **2**, and **3** belongs to polymer-coordinated, binuclear and mononuclear, respectively and all Schiff base ligands act as tridentate ligands. In vitro antibacterial study of compounds indicates that metal chelates have higher activity than respective ligands against Gram-Positive bacteria. Anticancer activity of compounds reveals that all metal compounds show better activity than respective ligands against AGS and SW174 cancer cell line and might be due to chelation theory.

References

[1] S. Yamada, *Coordination Chemistry Reviews*, 1 (1966) 415-437.

[2] L. H. A. Rahman, R. M. E. Khatib, L. A. E. Nassr, A. M. A. Dief, F. E. Lashin, *Spectrochim. Acta A*, 111 (2013) 266.

[3] L. H. A. Rahman, R. M. E. Khatib, L. A. E. Nassr, A. M. A. Dief, A. A. Seleem, *Spectrochim. Acta A*, 117 (2014) 366.

[4] X. G. Ran, L. Y. Wang, Y. C. Lin, J. Hao, D. R. Cao, *Appl. Organometal. Chem.*, 24 (2010) 741.

[5] O. Pouralimardan, A. Ch. Chamayou, Ch. Janiak, H. H. Monfared, *Inorganica Chimica Acta*, 360 (2007) 1599-1608.

[6] R. Bikas, M. Ghorbanloo, R. Sasani, I. Pantenburg, G. Meyer, *Journal of Coordination Chemistry*, 70 (2017) 819-830.

[7] B. I. N. Mladenova, G. T. Momekov, *Bulgarian Chemical Communications*, 49 (2017) 83-88.
[8] J. G. Deng, Y. Gou, W. Chen, X. Fu, H. Deng, *Bioorganic & Medicinal Chemistry*, 24 (2016) 2190-2198.
[9] G. Gomathi, R. Gopalakrishnan, *Materials Science and Engineering*, 64 (2016) 133-138.
[10] Y. Harinath, D. H. K. Reddy, B. N. Kumar, Ch. Apparao, K. Seshaiah, *Spectrochimica Acta Part A: Molecular and Biomolecular Spectroscopy*, 101 (2013) 264-272.
[11] A. Mahal, R. A. E. Halawa, S. A. Zabin, M. Ibrahim, M. A. Refai, T. Kaimari, *Journal of Organic Chemistry*, 3 (2015) 1-8.
[12] P. Dandawate, K. Vemuri, E. M. Khan, M. Sritharan, S. Padhye, *Carbohydrate Polymers*, 108 (2014) 135-134.
[13] M. A. Abdelgawad, M. B. Labib, M. A. Latif, *Bioorganic Chemistry*, 74 (2017) 212-220.
[14] L. Li, Y. Zh. Zhang, E. Liu, Ch. Yang, J. A. Golen, A. L. Rheingold, G. Zhang, *Journal of Molecular Structure*, 110 (2016) 180-184.
[15] S. Mondal, B. Pakhira, A. J. Blake, M. G. B. Drew, Sh. K. Chattopadhyay, *Polyhedron*, 117 (2016) 327-337.
[16] J. Qin, Sh. Sh. Zhao, Y. P. Liu, Zh. W. Man, P. Wang, L. N. Wang, Y. Xu, H. L. Zhu, *Bioorganic & Medicinal Chemistry Letters*, 26 (2016) 4925-4929.
[17] G. Xu, B. Tang, L. Gu, P. Zhou, H. Li, *Journal of Molecular Structure*, 1120 (2016) 205-214.
[18] U. P. Meshram, G. B. Pethe, A. R. Yaul, B. G. Khobragade, M. L. Narwade, *Journal of Physical Chemistry A*, 91 (2017) 1877-1882.
[19] E. I. Yousif, R. M. Ahmed, H. A. Hasan, A. S. A. Fahdawi, M. J. A. Jeboori, *Journal of Science and Technology*, 41 (2017) 103-109.
[20] Y. Zhang, L. Zhang, L. Liu, J. Guo, D. Wu, G. Xu, X. Wang, D. Jia, *Inorganica Chimica Acta*, 363 (2010) 289-293.
[21] J. G. Deng, W. Chen, H. Deng, *Journal of Fluorescence*, 26(2016) 1987-1996.
[22] Sh. Shen, H. Chen, T. Zhu, X. Ma, J. Xu, W. Zhu, R. Chen, J. Xie, T. Ma, L. Jia, Y. Wang, Ch. Peng, *Oncology Letters*, 13 (2017) 3169-3176.
[23] Y. Du, W. Chen, X. Fu, H. Deng, J. G. Deng, *Royal Society of Chemistry Advances*, 6 (2016) 109718-109725.
[24] M. E. Behery, H. E. Twigry, *Molecular and Biomolecular Spectroscopy*, 66 (2007) 28-36.
[25] R. Fekri, M. Salehi, A. Asadi, M. Kubicki, *Polyhedron*, 128 (2017) 175-187.
[26] A. Datta, N. T. Chuang, J. H. Huang, H. M. Lee, *Acta Crystallographica*, 65 (2009) 996.
[27] R. Fekri, M. Salehi, A. Asadi, M. Kubicki, *Applied Organometallic Chemistry*, (2017) 1-17.
[28] J. Zhou, Z. F. Chen, Y. S. Tan, X. W. Wang, Y. H. Tan, H. Liang, Y. Zhang, *Acta Crystallogr*. 60 (2004) 519.
[29] Agilent Technologies, Crys Alis PRO (Version 1.171.33.36d), Agilent Technologies Ltd, (2011).
[30] G. M. Sheldrick, *Acta Crystallogr*., (2015), C71, 3-8.
[31] C. S. Ukesh, S. D. Patil, *J. of Life Sciences*, 5 (2017) 97-101.

[32] F. Pakdel, Sh. Ghasemi, A. Babaloo, Y. Javadzadeh, R. Momeni, M. Ghanizadeh, S. R. Moaddab, F. Y. Fathi, *J. Clin Diagn Res.* 11 (2017) 16-19.
[33] R. F. M. Elshaarawy, Ch. Janiak, *Journal of chemistry*, 9 (2016) 825-834.
[34] A. Brezdent, M. F. Mohamed, M. Nepal, J. S. Harwood, J. Kuriakose, M. N. Seleem, J. Chmielewski, J. Am. Chem. Soc., 138 (2016) 10945-10949.
[35] J. Duan, J. Kang, T. Han, Y. Ma, Q. Guo, Y. Song, Q. Zhao, Y. Yang, R. Zhang, *Journal of Pharmaceutical Sciences*, 30 (2017) 551-553.
[36] S. Sujarani, A. Ramu, Journal of Molecular Structure, 1059 (2014) 299-308.
[37] R. Gomathi, A. Ramu, A. Murugan, *Bioinorganic Chemistry and Applications*, (2014) (2014) 1-12.
[38] N. Bai, Ch. Sh. Lai, K. He, Zh. Zhou, L. Zh. Quan, N. Zhu, Q. Y. Zheng, M. H. Pan, Ch. T. Ho, *J. Nat. Prod.*, 69 (2006) 531-535.
[39] F. Shokri, M. Heidari, S. Gharagozloo, M. G. Khansari, *Toxicology*, 146 (2000) 171-176.
[40] C. Batistakis, Y. Gan, C. J. Cardin, D. G. Paschalidis, C. A. Kavounis, Z. Kristallogr, *NCS*, 222 (2007) 251-252.
[41] M. Salehi, F. Rahimifar, M. Kubicki, A. Asadi, *Inorganica Chimica Acta*, 443 (2016) 28-35.
[42] B.G. Tweedy, *Phytopathology*, 55 (1964) 910.
[43] M. M. A. Aly, A. M. Salem, M. A. Sayed, A. A. A. Aziz, *Molecular and Biomolecular Spectroscopy*, 136 (2015) 993-1000.
[44] G. Jiang, Y. Jiang, Y. Shen, K. H. Nam, D. Lee, Zh. Gao, *International Journal of Pharmaceutics*, 365 (2009) 155-161.
[45] J. Dh. Chellaian, J. Johnson, *Molecular and Biomolecular Spectroscopy*, 127 (2014) 396-404.
[46] K. L. Haas, K. J. Franz, *Chem. Rev.* 109 (2009) 4921-4960.

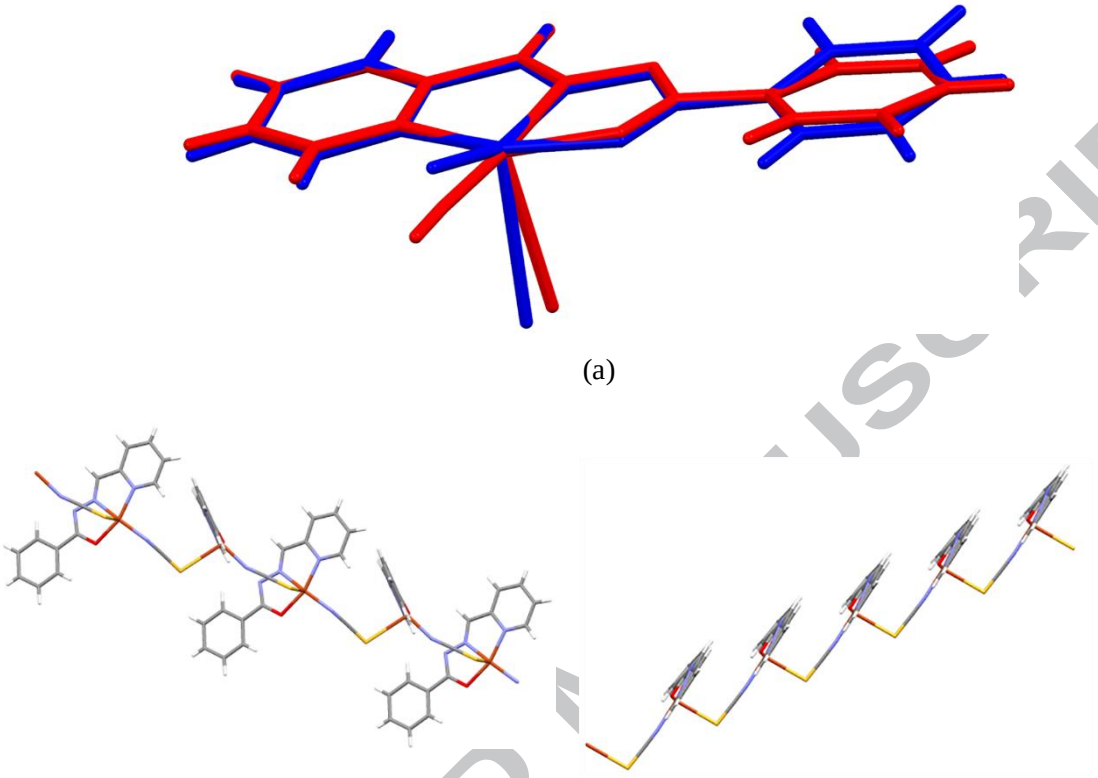

(a)

(b)

Fig. 1. Comparison of (a) the monomers in (**1**) and XIQLIT (cf. text), and (b) polymers formed in XIQLIT (left) and in (**1**) (right).

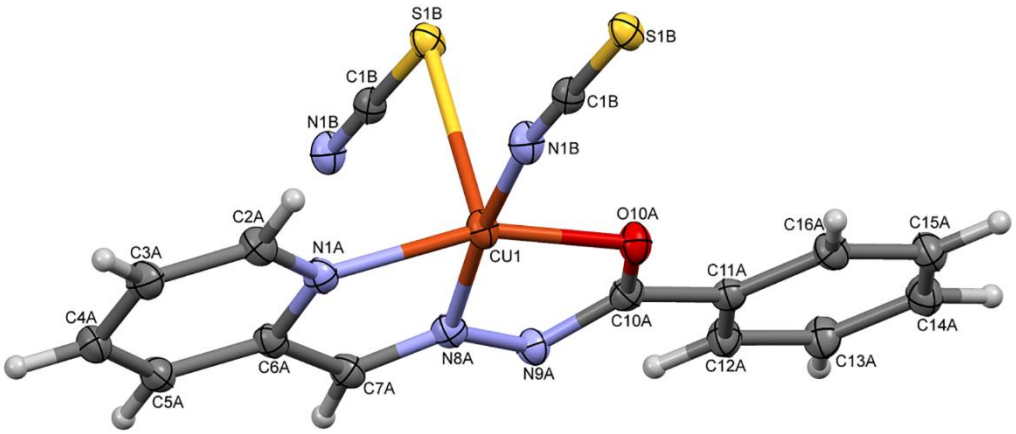

Fig. 2. A perspective view of the monomer complex in (**1**); ellipsoids are drawn at the 50% probability level and hydrogen atoms are shown as spheres of arbitrary radii.

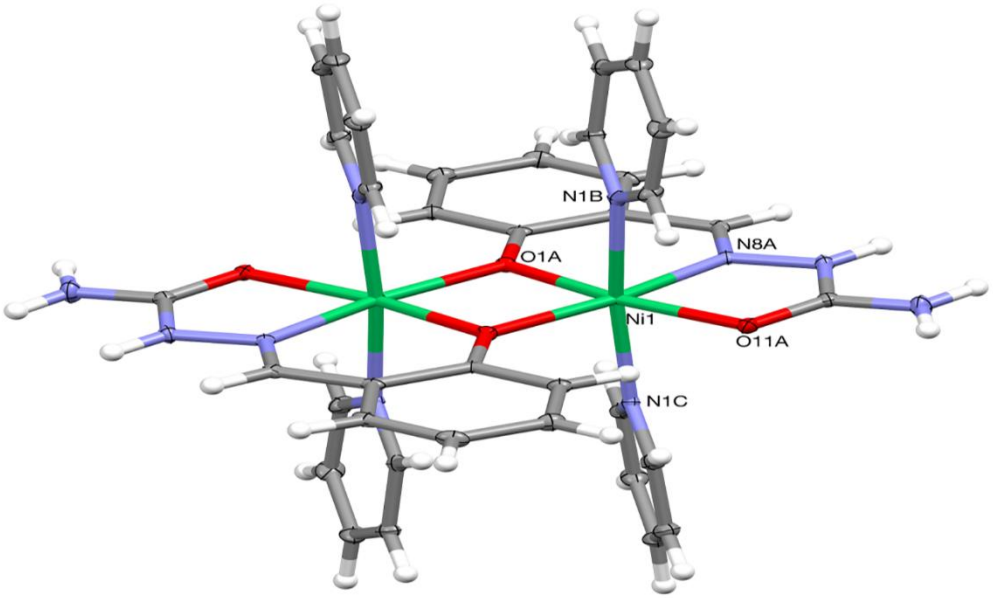

Fig. 3. A perspective view of the dimeric complex in (**2**); ellipsoids are drawn at the 50% probability level, hydrogen atoms are shown as spheres of arbitrary radii. Unlabelled part is related to the labeled one by symmetry operation 1/2-x,3/2-y,1/2-z.

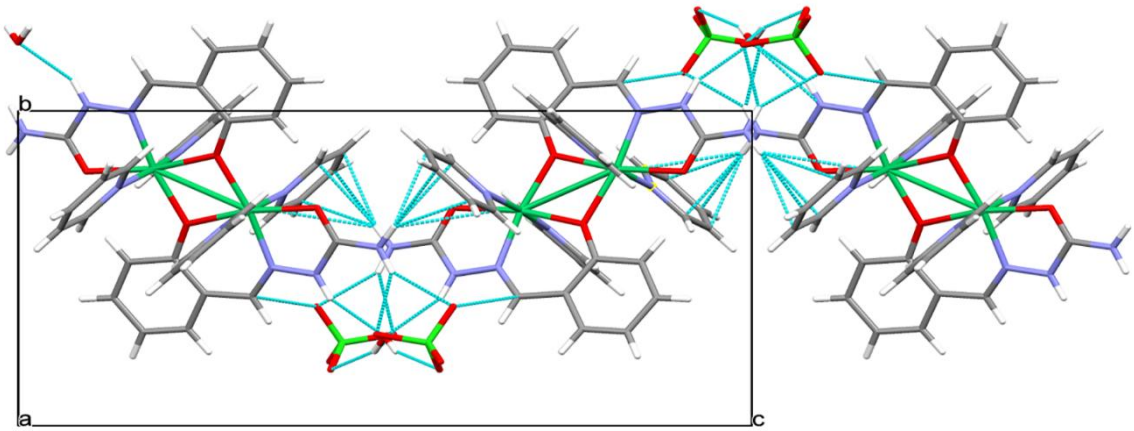

Fig. 4. Fragment of the hydrogen-bonded chain in (**2**) as seen along x-direction; hydrogen bonds are shown as blue dashed lines.

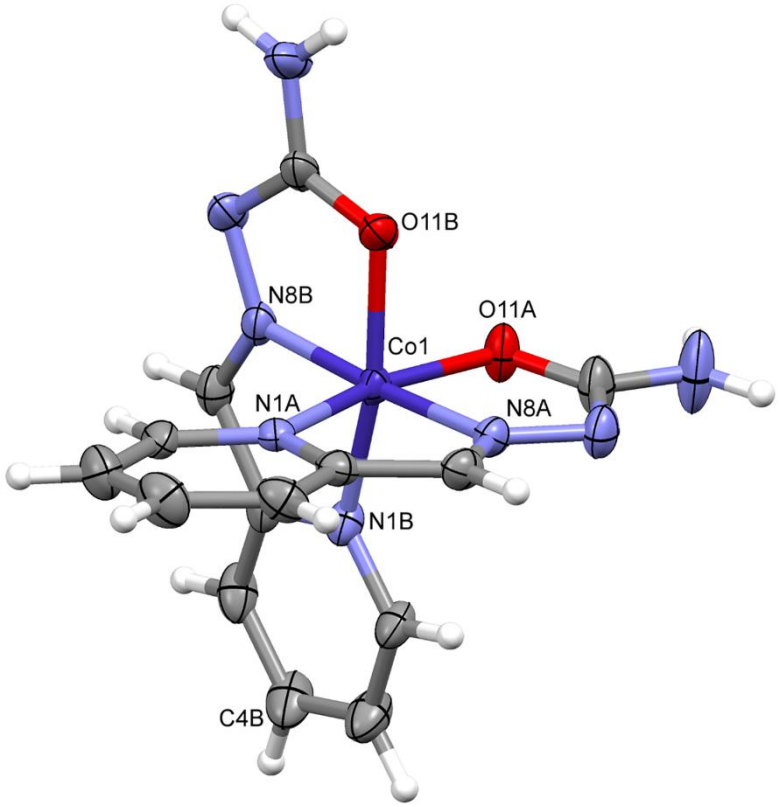

Fig. 5. A perspective view of the cationic complex in (**3**); ellipsoids are drawn at the 50% probability level, hydrogen atoms are shown as spheres of arbitrary radii.

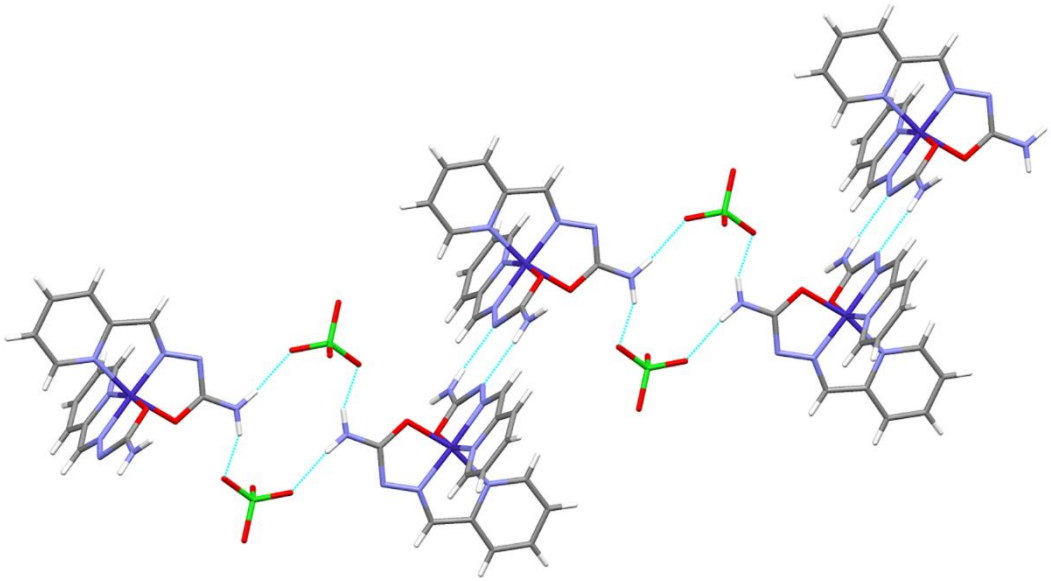

Fig. 6. Fragment of the hydrogen-bonded chain in (**3**); hydrogen bonds are shown as dashed blue lines.

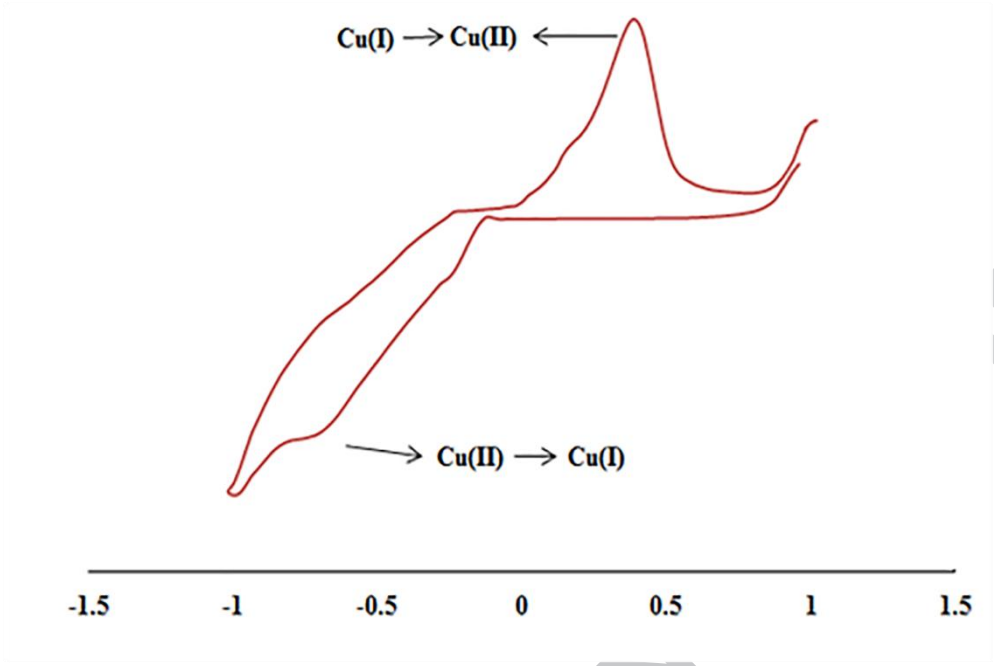

(a)

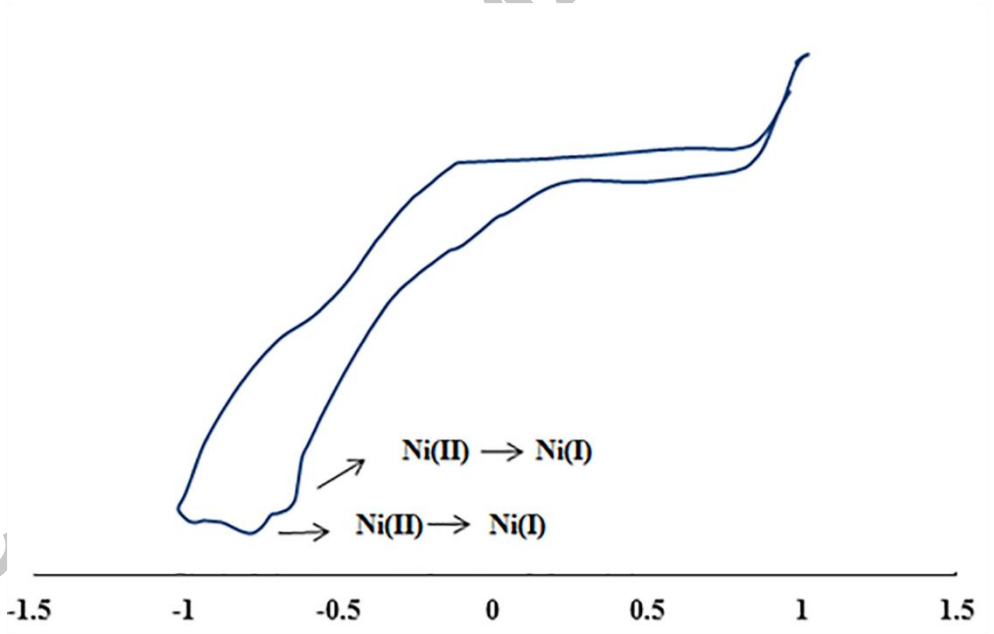

(b)

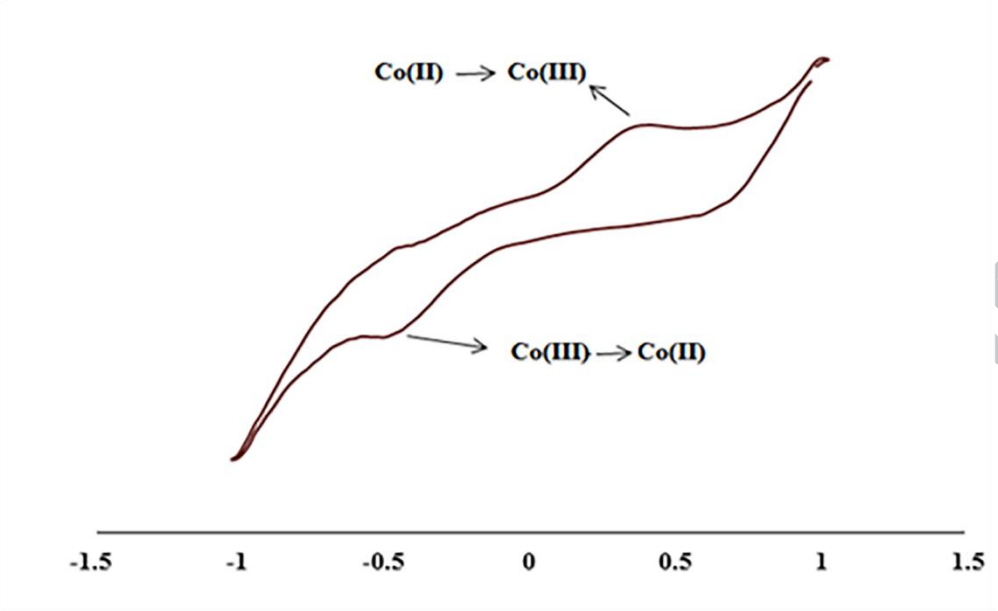

(c)

Fig. 7. Cyclic voltammograms of polymer **1** (a) and complexes of **2** (b) and **3** (c) in DMF (1×10^{-3}M).

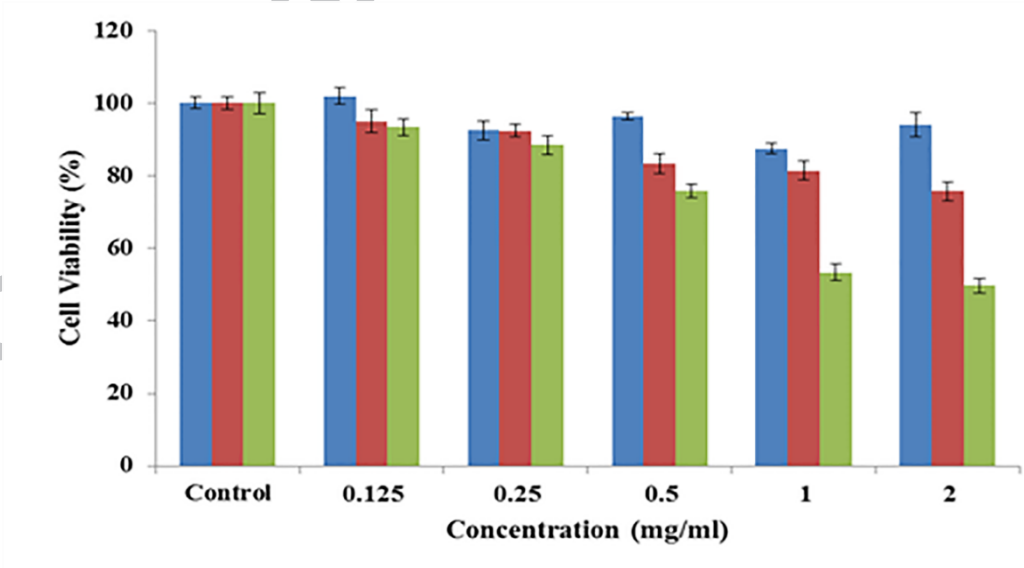

(a)

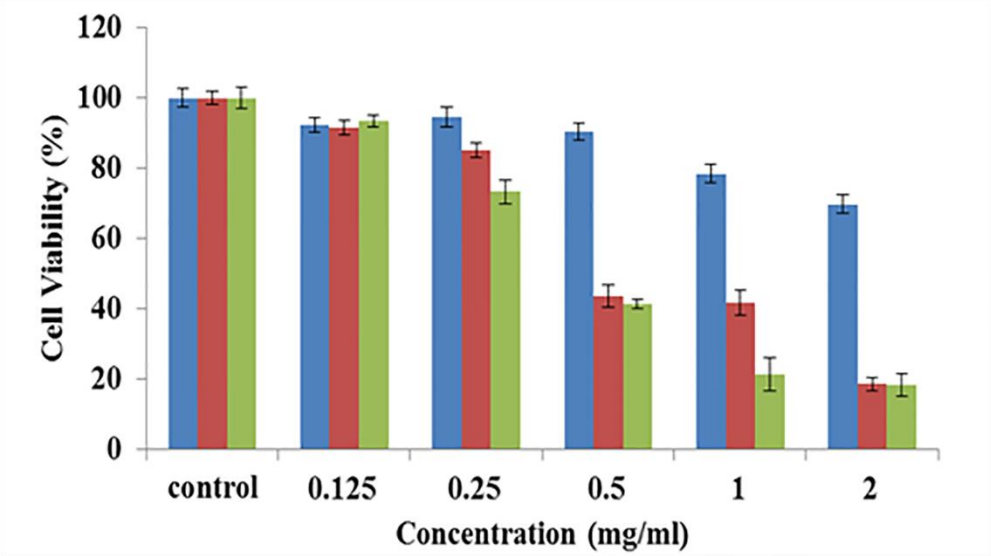

(b)

Fig. 8. Effect of Schiff base ligands (a) and their metal compounds (b) at different concentrations (0.125, 0.25, 0.5, 1 and 2 mg/ml) on the AGS cell line, (**HL**^{1}), **1** (green), (**H_2L^2**), **2** (red), (**HL**^{3}), **3** (blue).

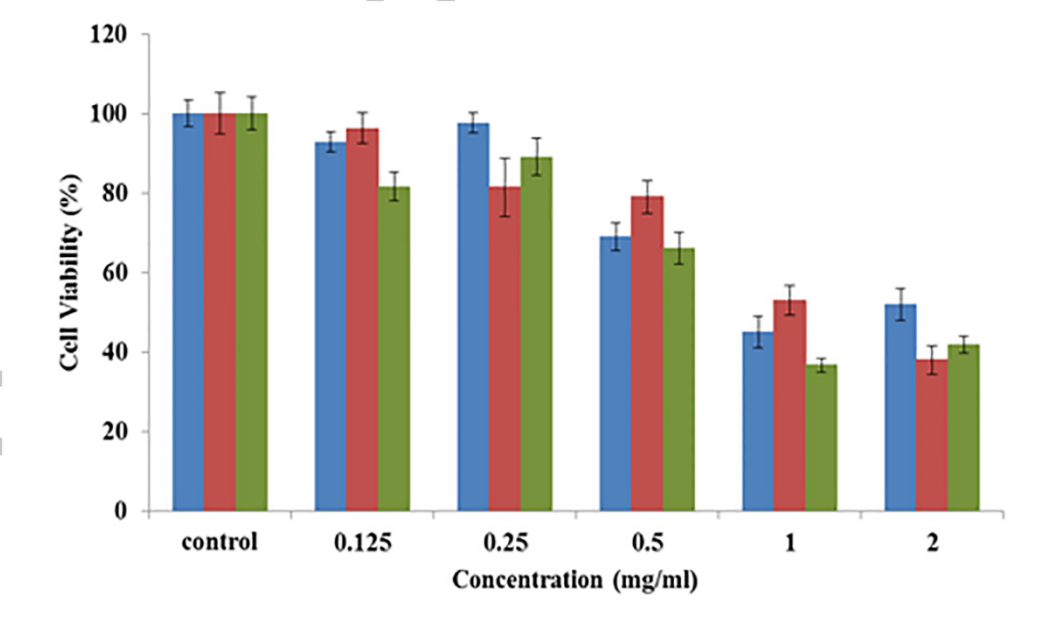

(a)

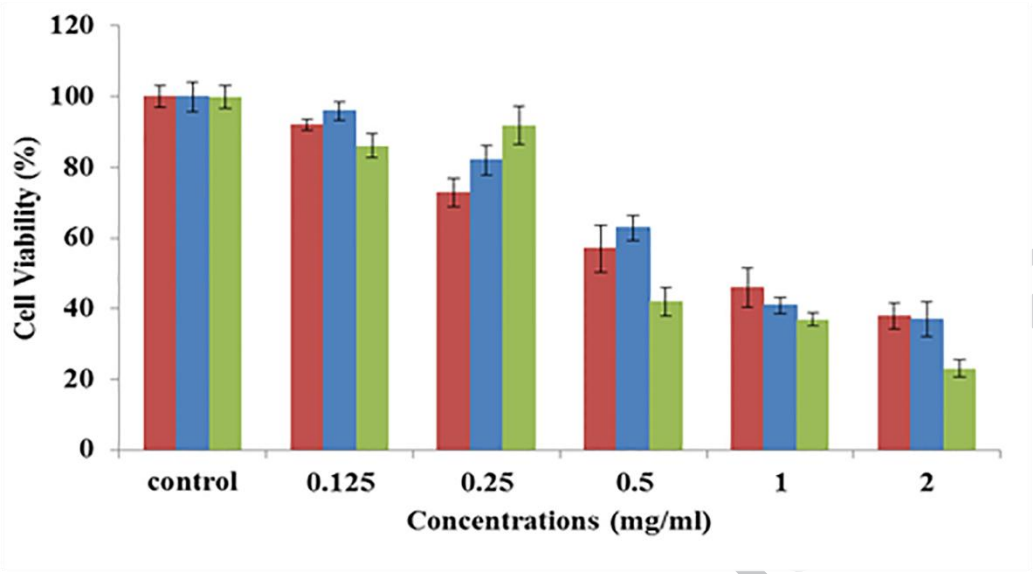

(b)

Fig. 9. Effect of Schiff base ligands (a) and their metal compounds (b) at different concentrations (0.125, 0.25, 0.5, 1 and 2 mg/ml) on the SW742 cell line, (**HL**^{1}), **1** (green), (**H$_2$L**^{2}), **2** (red), (**HL**^{3}), **3** (blue).

Table 1. Crystal data, data collection and structure refinement.

Compound	**1**	**2**	**3**
Formula	$[C_{14}H_{10}CuN_4OS]_n$	$[C_{36}H_{36}N_{10}Ni_2O_4]^{2+}\cdot 2(ClO_4)^-\cdot H_2O$	$[C_{14}H_{14}CoN_8O_2]^+\cdot ClO_4^-$
Formula	345.86	1007.08	484.71
Crystal system	monoclinic	monoclinic	triclinic
Space group	$P2_1/n$	$I2/a$	P-1
a(Å)	5.66016(12)	19.7348(4)	8.3696(5)
b(Å)	14.5908(3)	10.4539(2)	10.3786(5)
c(Å)	16.7539(4)	20.2919(4)	11.9066(6)
α (º)	90	90	106.261(4)
β(º)	94.970(2)	90.861(2)	104.568(4)
γ (º)	90	90	102.500(4)
V(Å^3)	1378.44(5)	4185.86(14)	914.02(9)
Z	4	4	2
D_x(g cm^{-3})	1.67	1.60	1.76
F(000)	700	2072	492
μ(mm^{-1})	3.686	1.104	9.216
Θ range (^{0})	4.02 – 76.26	3.59 – 26.65	4.10 – 76.59
Reflections:			
collected	6506	8292	7744
unique	2845 (0.020)	4029 (0.019)	3770 (0.044)
with	2610	3603	3513
R(F) [I>2σ(I)]	0.034	0.041	0.046
wR(F^2)	0.095	0.135	0.126
R(F) [all data]	0.037	0.046	0.049
wR(F^2) [all	0.098	0.141	0.129
Goodness of fit	1.08	1.11	1.08
max/min Δρ (e Å^{-3})	0.39/-0.53	2.28/-1.04	0.53/-0.56

Table 2. Relevant geometrical parameters (Å, °) with s.u.'s in parentheses. Line "angles" lists three largest angles around the metal center; A, B and C denote the least-squares planes of phenyl/pyridine ring, chain, and terminal ring in case of (**1**).

(1)		**(2)**		**(3)**	
Cu-N1A	2.031(2)	Ni-O1A	2.0299(18)	Co-N1A	1.914(2)
Cu-N8A	1.933(2)	Ni-O1A (*1/2-x,3/2-y, 3/2-z*)	2.0561(19)	Co-N1B	1.904(2)
Cu-O10A	1.9716(17)	Ni-N8A	2.011(2)	Co-N8A	1.860(2)
Cu-N1B	1.928(2)	Ni-O11A	2.0731(19)	Co-N8B	1.861(2)
Cu-S1B (*x-1,y,z*)	2.6819(7)	Ni-N1B	2.122(2)	Co-O11A	1.914(2)
		Ni-N1C	2.122(2)	Co-O11B	1.914(2)
Angles	173.20(9)		172.98(8)		176.10(10)
	157.44(8)		171.20(8)		166.19(9)
	100.83(8)		169.24(7)		165.92(10)
C7-N8-N9	123.8(2)		119.1(2)		125.2(3)
					125.7(3)
N8-N9-C10	107.14(19)		115.7(2)		107.5(2)
					107.4(2)
N1-C6-C7-N8	-0.3(3))	C1-C6-C7-N8	-0.8(4)	N1-C6-C7-N8	0.7(3)
					2.1(3)
C6-C7-N8-N9	-178.8(2)		176.5(2)		-179.193)
					-179.2(2)
C7-N8-N9-C10	-179.6(2)		177.2(2)		-175.4(3)
					-174.8(3)
N8-N9-C10-C11	-177.48(19)	N8-N9-C10-O11	-1.2(4)		1.3(5)
					-3.1(4)
N9-C10-C11-C12	7.2(3)	N8-N9-C10-N12	180.0(2)		179.4(3)
					177.6(3)
A/B	0.7(2)		4.32(18)		6.65(17)
					6.40(11)
B/C	9.2(2)				
A/C	8.61(12)				

Table 3. Hydrogen bond data (Å, °). Ctg1 describes centroid of the N1C pyridine ring.

D	H	A	D-H	H···A	D···A	D-H···A
			(2)			
N9A	H9A	O1E	0.88	2.12	2.906(3)	149
N12A	H12B	O2D^{i}	0.88	2.48	3.166(4)	135
N12A	H12B	O3D^{i}	0.88	2.34	3.057(3)	139
N12A	H12A	Cg1^{i}	0.88	2.42	3.238(3)	154
O1E	H1E	O1D	0.84	2.02	2.817(3)	159
			(3)			
N12A	H12A	O3C	0.88	2.17	2.931(4)	145
N12A	H12B	O4C^{ii}	0.88	2.15	2.999(4)	161
N12B	H12C	O3C^{iii}	0.88	2.58	2.992(3)	110
N12B	H12B	N9B^{iv}	0.88	2.04	2.915(4)	177

Symmetry codes: ^{i} ½-x,y,1-z; ^{ii} 1-x,-y,-z; ^{iii} -1+x,y,z; ^{iv} –x,1-y,1-z.

Table 4. The MIC and MBC values of the synthesized compounds (10^{-6} M).

pound	Gram-Positive Bacteria				Gram-Negative Bacteria			
	B. subtilis		S. aureus		K. pneumoniae		E. coli	
	MBC	MIC	MBC	MIC	MBC	MIC	MBC	MIC
HL^{1}	444	111	444	222	444	222	444	444
1	3.5	1.7	7.0	0.8	56.6	28.3	56.6	56.6
H$_2$L^{2}	558	279	558	279	558	558	558	558
2	8.0	4.0	15.8	1.9	63.4	15.8	63.4	63.4
HL^{3}	609	304	609	304	609	304	609	609
3	32.3	8.0	64.7	16.1	129	64.7	129	129

* Three metal complexes from hydrazone Schiff base ligands were synthesized and characterized.

* Molecular structures of the metal compounds were determined by single crystal X-ray diffraction technique.

* The cyclic voltammetry behavior of these compounds was discussed.

* The Schiff base ligands and their metal compounds have been screened for their antibacterial and in vitro anticancer activities.

In this paper, metal chelates of Schiff base derived from hydrazones have been prepared and characterized by ^{1}HNMR, IR, UV-Vis spectroscopy and cyclic voltammetry. Single crystal X-ray crystallography studies confirm the structure of newly synthesized Schiff bases. The Schiff bases act as tridentate ligands. The free ligands and metal compounds are screened for their antibacterial activities against Gram-positive and Gram-negative bacteria. Further the cytotoxic effect of the ligands and their metal compounds examined on cancer cell lines showed that the metal compounds exhibit better activity than ligands.